

CHARACTERIZATION OF THERMAL PROPERTIES OF POROUS SILICON FILM/SILICON USING PHOTOACOUSTIC TECHNIQUE

Q. Shen^{*} and *T. Toyoda*

Department of Applied Physics and Chemistry, The University of Electro-Communications,
1-5-1 Chofugaoka, Chofu, Tokyo 182-8585, Japan

Abstract

We have applied photoacoustic (PA) technique to study the thermal properties of porous silicon (PS) films formed on *p*-type Si substrates by electrochemical anodic etching. Four PS samples with close thicknesses but greatly different porosities (from 20 to 60%) were examined. From the dependences of the PA signals on the modulation frequency of excitation light measured under a transmission detection configuration (TDC), effective thermal diffusivities for the two-layered PS/Si samples were determined and found to decrease greatly from 0.095 to 0.020 cm² s⁻¹ as the porosity increased from 20 to 60%.

Keywords: carrier diffusion, photoacoustic technique, porosity, porous silicon, thermal diffusion, thermal diffusivity

Introduction

Since porous silicon (PS) was found to show efficient luminescence at room temperature in 1990 [1], a strong interest has been focused on both the light emission mechanism and the applications of PS in light emitting devices and optoelectronic devices [2]. Another potential application of PS is to use it as a thermal insulator in thermal effects microsystems, because of its low thermal conductivity. It is very important and necessary to study the optical and thermal properties of PS for these applications. In particular, it is desirable to measure the properties of PS in situ without separating PS from the Si substrate. Photoacoustic (PA) technique is a photothermal detection method, which has proved to be powerful for investigating optical, electronic and thermal properties of materials by measuring the non-radiative de-excitation processes that follow the optical absorption [3–5]. One important merit of the PA technique is that it is a non-contact and non-destructive method requiring no particular sample treatment. In an earlier paper, we reported our experimental results on the influence of chemical etching by low concentration hydrofluoric acid (HF) for electrochemical anodized PS samples on its optical

* Author for correspondence: E-mail: shen@pc.uec.ac.jp.

absorption using PA technique [6]. It was demonstrated that the PA measurement was useful for studying the optical absorption properties of PS in-situ on the Si substrate. We also applied the PA method under a transmission detection configuration (TDC) to study the thermal and electronic transport properties of CdInGaS₄ [7, 8]. We found that the PA signal in the TDC originated from both electronic transport process and heat transport process in the semiconductor sample, and these two processes could be separated by changing the modulation frequency of the excitation light. We determined the values of the excess-carrier lifetime, carrier diffusivity, surface recombination velocity and thermal diffusivity of the CdInGaS₄ by fitting theoretical calculation results to the experimental results [8].

In this paper, we applied the PA method under TDC to study the thermal property of the PS film/Si two-layered samples. We will report our experimental results on the measurements of thermal diffusivities of PS samples with different porosities from 20 to 60%. We will show how the thermal diffusivity of PS is influenced with the porosities of the PS.

Experimental

PS layers were formed on *p*-type, boron-doped, (100)-oriented Si substrates (thickness: 500 μm) of 5–15 Ω cm resistivity by electrochemical anodic etching in a HF (47%)–water solution [6]. A Pt film sputtered on the unpolished surface of the Si was used as the electrode. The anodization current density was 10 mA cm⁻². Four PS samples were prepared with different anodization times, i.e., (a) 15, (b) 30, (c) 45 and (d) 60 min. The thickness of the four samples was measured to be 26.6, 27.2, 28.3 and 30.0 μm, respectively, using scanning electronic microscope (SEM) images. Figure 1 shows an example of the SEM image for sample (c). The mass changes Δ*M* of each Si wafer before and after the electrochemical anodic etching was measured and the porosities *P* were calculated by

$$P = \frac{\Delta M}{hS\rho} \quad (1)$$

where *S*, ρ and *h* were the anodic etching area of the Si wafer and the density of the Si wafer (i.e., 2.33 g cm⁻³) and the thickness of the PS film, respectively. Thus the poros-

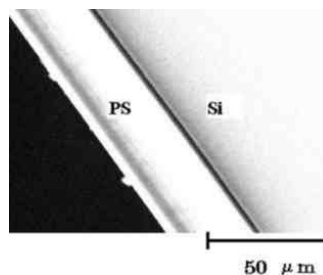


Fig. 1 A scanning electronic microscope (SEM) image of the cross section of a PS/Si sample prepared with the anodization time of 45 min at a current density of 10 mA cm⁻²

ities of the four samples were determined to be 23, 37, 52 and 61%, respectively. Figure 2 shows the dependences of the thickness h and porosity P of the PS films on the anodization time. It can be seen that the PS film thickness changed a little but the porosity increases greatly with the increase of the anodization time from 15 to 60 min under our experimental conditions.

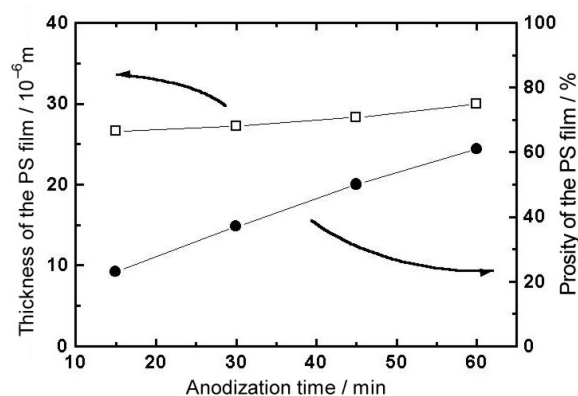


Fig. 2 Dependences of the PS film thickness and porosity on the anodization time

A gas-microphone equipment was used for the photoacoustic measurement [3, 9]. A 300 W xenon arc lamp was used as the light source. A monochromatic light beam was obtained by passing the light through a monochromator. Then the light was modulated with a mechanical chopper and focused on the surface of a sample placed inside a sealed PA cell. The PA cell was an aluminum cylinder with a small channel at its periphery in which a microphone was inserted. The inside volume of the cell was approximately 0.5 cm^3 . The cell was suspended by four rubber bands to prevent outside vibration. The cell window had a high transparency throughout the observed wavelength range and the sample holder could be easily removed from the cell. The light absorbed by the sample converts into heat by non-radiative relaxation processes and results in a pressure fluctuation of the air inside the cell. The pressure fluctuation oscillating at the chopper frequency was detected by the microphone enclosed in the PA cell and amplified by a preamplifier. Finally the PA signal intensity and phase were detected by a two-phase lock-in amplifier and recorded on a computer. Measurement of the PA spectra was carried out in the wavelength range of 320–1200 nm. The modulation frequencies used for the PA spectroscopic measurement were 33 and 333 Hz. The PA spectra were normalized using the PA signals from a carbon black sheet [9]. The modulation frequency dependence of the PA signal intensity at fixed photon energy points in the spectra was measured in the range of 12–400 Hz. The experiments were carried out at room temperature.

Results and discussion

Figure 3 shows an example of the PA intensity spectra of the PS film/Si samples (sample (d)). In Fig. 3, the PA signals measured under a modulation frequency of 33 Hz increased at the photon energy (PE) of 1.1 and 2.0 eV, respectively. Similar results were obtained for the other samples. The PA signal from the 1.1 eV excitation was due to optical absorption of the Si substrate beneath the PS films and the PA signal from 2.0 eV toward the higher energy was considered to be mainly due to the optical absorption from the PS film. However, only the PA signal due to optical absorption from the PS film was observed when the modulation frequency increased up to 333 Hz as shown in Fig. 3. It is known that the PA signal arises from optical absorption within a thermal diffusion length μ ($\mu = \sqrt{\alpha/\pi f}$ where α is the thermal diffusivity and f is the modulation frequency). It means that the thermal diffusion length μ is inversely proportional to the square root of modulation frequency f . So the PA spectra shown in Fig. 3 means that the thermal diffusion length is larger than the thickness of the PS layer at a modulation frequency of 33 Hz but smaller than that of the PS layer at a modulation frequency of 333 Hz. The blue shift of the optical band gaps of the PS layers from that of crystal Si (1.1 eV) indicates a stronger quantum confinement of carriers in the PS layers due to the smaller dimension of the PS microcrystallites.

Figure 4 shows the experimental arrangement for PA detection in a transmission detection configuration (TDC). Figure 5 shows the dependences of the PA signal intensities of PS/Si samples on the light modulation frequencies for four samples measured under the TDC (as shown in Fig. 4), i.e., the irradiation of light was from the surface of PS layer and the detection of the PA signal was from the Si surface [8, 10]. The excitation wavelength was 400 nm, i.e. the excitation photon energy (3.1 eV) is much larger than the lowest excitation energy of the PS films (about 2.0 eV). The optical absorption can be assumed to be taking place at the PS surface. As shown in Fig. 5, for each sample, the PA signal intensity decreased with the increase of the

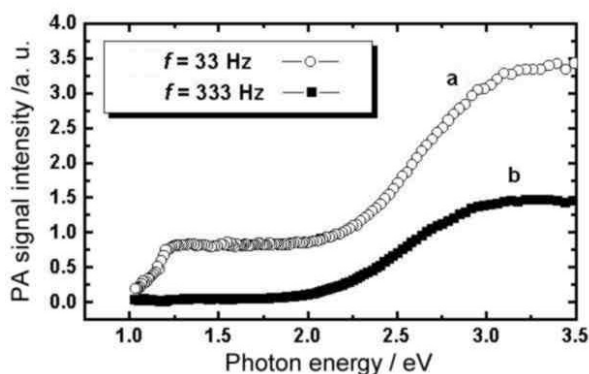


Fig. 3 PA intensity spectra for a PS/Si sample (sample (d): anodization time of 60 min) measured with the light modulation frequencies of a – 33 and b – 333 Hz

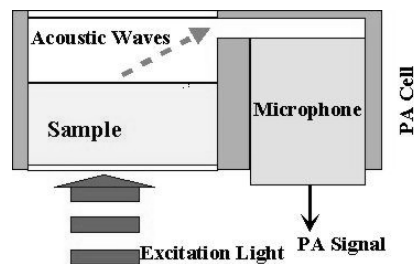


Fig. 4 Experimental arrangement for PA detection in the transmission detection configuration (TDC)

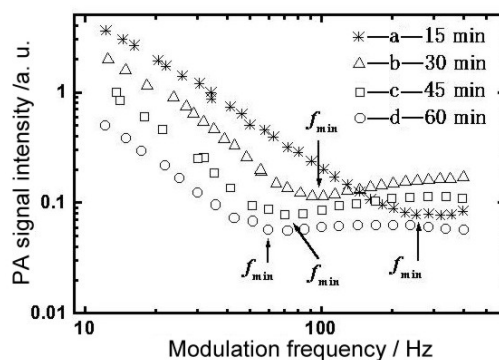


Fig. 5 Dependence of the photoacoustic signal intensity of PS film/Si samples on modulation frequency in TDC for samples a – 15, b – 30, c – 45, and d – 60 min. The wavelength of the excitation light is 400 nm

modulation frequency and showed a minimum at a frequency (f_{\min}). The minimum in the PA signal intensities of the PS film/Si samples moved to lower frequency region with the increase of anodization time during the electrochemical anodic process. The minimum frequency (f_{\min}) were about 273, 97, 71 and 60 Hz for the samples (a), (b), (c) and (d), respectively.

By theoretical analyses and experimental results, we have known that the PA signals obtained in TDC were attributed to both the thermal diffusion and carrier transport processes for semiconductor materials [8, 10]. For the frequency region lower than the frequency f_{\min} , the samples were thermally thin and the ‘thermal wave’ components caused by the heat sources generated at the irradiated surface were dominant. For higher frequencies than f_{\min} , the sample was thermally thick and the carrier transport contribution to the PA signals, i.e., the heat source generated at the rear surface by non-radiative recombination of the carrier was predominant. In this way, the PA signals in TDC were attributed to a thermal diffusion process or a carrier diffusion process by controlling the modulation frequency. If the sample is homogeneous, the frequency dependence of the PA signal intensity resulted from the thermal diffusion process in TDC for $f < f_{\min}$ was governed by $e^{-L\sqrt{\pi f/\alpha}}/f = e^{-L/\mu}/f$, where μ is the thermal diffusion length for frequency f and L is thickness of the whole sample. At the fre-

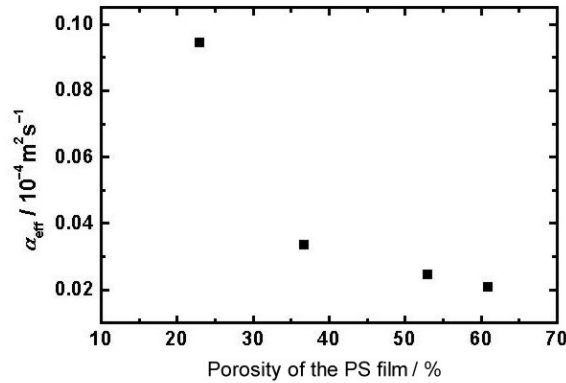


Fig. 6 Dependence of the effective thermal diffusivity α_{eff} of the PS/Si two-layered samples on the PS film porosity

quency f_{min} , the PA signal resulted from the thermal wave became so small that it can be ignored. It means that $e^{-L/\mu} \approx 0$, i. e., L/μ is roughly five for $f=f_{\text{min}}$. So it can be known that the sample thermal diffusion length μ_s became approximately five times smaller than the sample thicknesses L at f_{min} [8, 10].

For PS/Si two-layered sample, it is important to determine the pure thermal properties of the PS layers. However, the evaluation of the effective thermal property for the two-layered samples is also very important and necessary, since the two-layered sample will be used for practical applications. Here, we considered the PS/Si two-layered sample as a homogenous sample effectively with a thickness of H , in which $H=h_{\text{Si}}+h_{\text{PS}} \approx h_{\text{Si}}$ ($h_{\text{Si}} \gg h_{\text{PS}}$), h_{Si} and h_{PS} are thicknesses of the Si substrate and PS layer, respectively. Then the effective thermal diffusivities α_{eff} for the PS/Si two-layered samples could be estimated from f_{min} as 0.095, 0.034, 0.025 and 0.021 $\text{cm}^2 \text{ s}^{-1}$ from the analysis [8, 10] for samples (a), (b), (c) and (d), respectively. These values agree with those reported previously [11]. As mentioned above, the PS film thickness changed a little but the porosity changed largely with the anodization time for the four samples as shown in Fig. 2. Thus, the differences of the thermal diffusivity for the four samples were mostly due to the difference in the porosity. As shown in Fig. 6, the effective thermal diffusivity became smaller with the porosity of the PS layer became larger. The smaller effective thermal diffusivities mean that the thermal diffusivities of the PS films are much smaller than that of the Si substrate ($\sim 0.89 \text{ cm}^2 \text{ s}^{-1}$). This is because of the small dimensions of the PS structures and the presence of the air inside pores.

Summary

In summary, the PA technique has proved to be useful for studying the thermal properties of PS layers deposited on Si substrates in a non-contact and non-destructive manner. The PA intensity spectra confirmed a strong confinement effect occurring in the PS films from the blue shift of the lowest excitation energy compared with that of the crystal Si

(1.1 eV). The effective thermal diffusivities α_{eff} of the PS/Si two-layered samples were determined from the dependence of the PA signal intensities on the modulation frequencies of the excitation light under TDC. The α_{eff} was much smaller than that of the crystal Si and decreased with the increase of the porosity of the PS layer. It means that the thermal diffusivity of the PS films can be controlled by changing its porosity and the PS works as a thermal insulator in devices. Characterization of the thermal property of the pure PS film is being studied by establishing a two-layered model.

* * *

The authors thank Mr. T. Yamazaki and Mr. K. Torai for their help in the preparation of the samples and the measurements of the structures using scanning electronic microscopy

References

- 1 L. T. Canham, *Appl. Phys. Lett.*, 57 (1990) 1046.
- 2 D. Kovalev, H. Heckler, G. Polisski and F. Koch, *Phys. Stat. Sol. (b)*, 215 (1999) 871.
- 3 A. Rosencwaig, *Phys. Today*, 28 (1975) 23.
- 4 A. Rosencwaig, *Photoacoustic and Photoacoustic Spectroscopy*, Wiley, New York 1980, p. 1.
- 5 D. P. Almond, *Photothermal Science and Techniques*, Chapman & Hall 1996, p. 119.
- 6 T. Toyoda, T. Takahashi and Q. Shen, *J. Appl. Phys.*, 88 (2000) 6444.
- 7 Q. Shen and T. Toyoda, *Jpn. J. Appl. Phys.*, 39 (2000) 511.
- 8 Q. Shen and T. Toyoda, *Jpn. J. Appl. Phys.*, 39 (2000) 3146.
- 9 T. Toyoda and S. Shimamoto, *Jpn. J. Appl. Phys.*, 37 (1998) 2827.
- 10 M. D. Dramicanin, Z. D. Ristovski, P. M. Nikolic, D. G. Vasiljevic and D. M. Todorovic, *Phys. Rev. B*, 51 (1995) 14226.
- 11 I. Delgadillo, A. Cruz-Orea, H. Vargas, A. Calderon, J.-J. Alvarado-Grill and L. C. M. Miranda, *Opt. Eng.*, 36 (1997) 343.